Journal of Applied Polymer Science

Uniform mPEG-*b*-PMETAC enables pH-responsive delivery of insulin

Zongjun Li, Yifei Zhang, Diannan Lu, Zheng Liu
Key Lab for Industrial Biocatalysis, Ministry of Education, Department of Chemical Engineering, Tsinghua University, Beijing 100084, China
Correspondence to: D. Lu (E-mail: ludiannan@tsinghua.edu.cn) and Z. Liu (E-mail: liuzheng@mail.tsinghua.edu.cn)

ABSTRACT: A cationic block copolymer (mPEG-*b*-PMETAC) with uniform molecular weight was synthesized using atom transfer radical polymerization. Insulin was reversibly encapsulated by mPEG-*b*-PMETAC via electrostatic interaction. The secondary and tertiary structures of insulin during the assembly and delivery processes were monitored by circular dichroism and fluorescence spectrum. The effects of pH and salt concentration on encapsulation were examined, respectively. Enhanced stability of the encapsulated insulin against proteolysis by trypsin and chymotrypsin was demonstrated. Insulin can be encapsulated and delivered from an mPEG-*b*-PMETAC assembly by tuning the pH and ionic strength, which determines the electrostatic interaction between insulin and the polymer.
© 2015 Wiley Periodicals, Inc. J. Appl. Polym. Sci. **2015**, *132*, 42596.

KEYWORDS: bioengineering; hydrophilic polymers; proteins

Received 26 March 2015; accepted 8 June 2015
DOI: 10.1002/app.42596

INTRODUCTION

Drug delivery systems have gained wide interest, particularly protein and peptide drugs which have marginal stability and lose their activity due to proteolysis and renal exclusion.[1] Targeted release is also expected for a full display of the function of protein drugs. To achieve these objectives, increased efforts in the fabrication of nanostructured drug delivery systems such as liposomes,[2] microspheres,[3] nanogels,[4] and polymeric micelles have been observed.[5,6] Kataoka and Harada[7] first reported that polyelectrolyte could reversibly form an assembly with proteins and DNAs through electrostatic interactions. Amphiphilic and neutral-ionic block co-polymers can also spontaneously form an assembly with counter-charged macromolecules in aqueous solution, forming a core–shell or core–corona structure.[8] The assembly of lysozyme and poly(ethylene glycol)–poly(ethylene glycol)–poly(α,β–aspartic acid) block copolymer [PEG-P(Asp)] can be tuned by altering pH and ionic strength, and behaves as an on-off control of activity.[9] It is reported that tumor tissues usually appear acidotic due to increased glucose consumption, and the extracellular pH of human tumors can reach 5.7.[10] This stimulated the e of pH-responsive drug delivery systems for antitumor drug delivery.[11,12] The abovementioned polyelectrolyte micelle systems, in which the formation and dissociation of the micelles can be conveniently tuned by pH, hold great promise for such pH-responsive protein and peptide drug delivery systems. However, the mechanism by which the polyelectrolytes affect the structure and function of encapsulated proteins or DNAs is not fully understood, particularly at the molecular level.

The high surface charge density of polyions with quaternary ammonium makes them attractive for use as drug carriers for cells or tissues.[13] While amphiphilic polymers grafted with quaternary ammonium and palmitoyl groups have been proposed for the oral administration of protein,[14,15] the hydrophobic interaction may lead to unfolding of encapsulated insulin and, consequently, accelerated degradation by chymotrypsin. PEG is a biocompatible polymer, which forms vast numbers of hydrogen bonds with water and thus enhances protein structure.[16] In fact, polymers with PEG block and quaternary ammonium groups have been used for gene delivery.[17,18] In this study, we synthesized a block polymer consisting of PEG and quaternary ammonium blocks, using the atom transfer radical polymerization (ATRP) procedure to achieve a uniform encapsulation suitable for the targeted and controlled delivery of insulin.

The purpose of this work was to develop new polyions suitable for the targeted oral administration of protein drugs. To achieve this objective, first, the polyions should be positively charged to ensure that they target cells or tissues with a negative surface charge. Second, the encapsulated protein should be protected against cleavage by trypsin or chymotrypsin. Finally, the delivery can be triggered by pH. Moreover, we attempted the ARTP procedure with a uniform distribution of polyions which favors the encapsulation and delivery of protein drugs.

Additional Supporting Information may be found in the online version of this article.
© 2015 Wiley Periodicals, Inc.

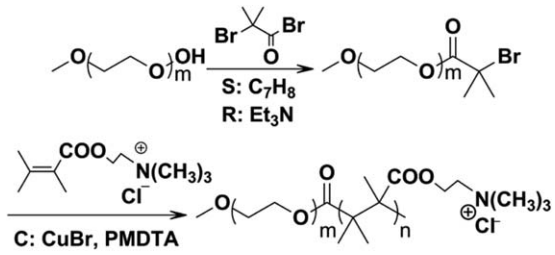

Figure 1. Synthesis of PEG-b–PMETAC by ATRP.

In this study, poly(ethylene glycol) mono-methylether-block–poly (2-(methacryloyloxy) ethyltrimethylmmonium chloride) (mPEG-*b*–PMETAC) was synthesized using ATRP. The potential of this polymer to construct a pH-responsive drug delivery system was tested using insulin as a model protein. The effects of pH and salt on the electrostatic interaction and hydrophobic interactions between this novel cationic block polymer and insulin were examined, respectively. The conformational change of insulin in relation to its secondary and tertiary structure during encapsulation and release were monitored. The stability of encapsulated insulin against enzymatic degradation was demonstrated.

EXPERIMENTAL

Chemical Agents

2-(Methacryloyloxy) ethyltrimethylammonium chloride (METAC, 72% aqueous solution), polyethylene glycol monomethylether ($M_w \sim 1900$), 2-bromoisobutyryl bromide, 1,1,4,7,7-pentamethyldiethylenetrilamine (PMDTA), and trifluoroacetic acid were purchased from Alfa Aesar Company (UK). Porcine insulin (28.6 IU/mg) was obtained from Wanbang Biopharmaceuticals (China). Trypsin and copper(I) bromide were purchased from Sigma-Aldrich Company (USA). Chymotrypsin was purchased from Amresco Company (USA). The Micro BCA protein assay kit was obtained from Beyotime Institute of Biotechnology (China). All other chemicals used were of analytical grade.

Synthesis of mPEG-*b*–PMETAC

A hydrophilic and positively charged block polymer, mPEG-*b*–PMETAC, was synthesized using ATRP, as shown in Figure 1.

The macromolecular initiator, poly(ethylene glycol) monomethyl ether-2-bromoisobutyrate (mPEG-Br), was synthesized as shown in Figure 1. In brief, 3.8 g mPEG ($Mw = 1900$) was first dissolved in 100 mL of anhydrous toluene. Then 0.28 mL triethylamine and 0.3 mL 2-bromoisobutyryl bromide were added. The reaction proceeded for 5 h at 45°C in an N_2 atmosphere. After filtering out insoluble substances, the solution was concentrated in a rotary subatmospheric evaporator at 40°C and precipitated in cold ether. The precipitate was dissolved in CH_2Cl_2, and then precipitated in cold ether. This dissolution–precipitation cycle was repeated three times before vacuum drying.

Then mPEG-*b*–PMETAC was synthesized by the ATRP method. Briefly, 0.23 g (~1.0 mmol) mPEG–Br and 9.4 mL (~50 mmol) 2-(methacryloyloxy) ethyltrimethylammonium chloride (METAC) was dissolved in 20 mL water in a Schlenk flask. After adding 151 mg (1.0 mmol) CuBr and 173 mg (1.0 mmol) 1,1,4,7,7-pentamethyldiethylenetrilamine (PMDTA) as ligand, the Schlenk flask was sealed. The mixture was degassed via a freeze–pump–thaw cycle three times and then incubated in an oil bath at 50°C for 24 h. After polymerization, the mixture was cooled to room temperature and dialyzed in water for 24 h to remove excess small molecules. The resultant solution was freeze-dried to obtain the solid polymer.

Encapsulation of Insulin in mPEG-*b*–PMETAC Micelles and Determination of Complexation Efficiency

First, 0.5 mL of solution A (10 mg mL^{-1} mPEG-*b*–PMETAC) was added to 4.5 mL of buffer solutions with increasing pH from 3.0 to 8.0 (Gly-HCl buffer 50 mM, pH 3.0; citrate buffer 50 mM, pH 4.0 and 5.0; phosphate buffer 50 mM, pH 6.0 and 7.0; Tris–HCl buffer 50 mM, pH 8.0), followed by the addition of 5 mL solution B containing 8 mg mL^{-1} insulin. The mixtures were vortexed and sonicated for 5 min, and then incubated overnight at room temperature.

The mixture was centrifuged at 11,000 rpm for 20 min. The supernatant containing the nonassociated insulin was collected, and the amount of free insulin was determined by the bicinchoninic acid (BCA) colorimetric protein assay.[19] The complexation efficiency was calculated using the following equation:

$$\text{Complexation efficiency}(\%) = \frac{(\text{Total insulin} - \text{Free insulin})}{\text{Total insulin}} \times 100\%$$

Enzymatic Degradation of Encapsulated Insulin

Trypsin (1.2 mg/mL) and chymotrypsin (0.16 mg/mL) were dissolved in Tris–HCl buffer (pH = 8.0, 50 mM, with 1 mM $CaCl_2$), respectively, as protease solutions. Solutions of insulin and insulin–polyelectrolyte complexes were divided into samples of 1 mL, each containing 0.2 mg insulin. Trypsin solution (30 μL) or chymotrypsin solution (40 μL) was added to each sample at 37°C for enzymatic degradation.[20] Aliquots (100 μL) were withdrawn at 0 min, 10 min, 30 min, 1 h, 2 h, and 3 h, respectively, stored at 4°C and the reaction was terminated by 1% trifluoroacetic acid aqueous solution. The samples were then centrifuged and the concentrations of the remaining insulin in the supernatant were measured by reverse phase chromatography (Shim-pack VP-ODS C18 (150), SHIMADZU Corporation, Japan) with distilled-deionized water (A) and acetonitrile (B), each containing 0.1% trifluoroacetic acid as the mobile phase. The gradient eluting agent was set as follows: 0–40 min: B10–60%; 40–45 min: B60%; 45–55 min: B10%.

Assays

Dynamic Light Scattering Measurements. The size of the micelles was determined using dynamic light scattering (DLS) measurements with a ZetaSizer 3000HSA (Malvern Instruments) and He–Ne lasers (22 mW) with wavelengths of 632.8 nm. All measurements were performed with a scattering angle of 90° at 298 K. Prior to DLS measurements, each sample was filtered using a 0.45 μm filter.

Stop-Flow Measurement of the Mixture Operation. The kinetics of the co-assembled insulin and mPEG-*b*–PMETAC were determined with the stop-flow modulation of the Chirascan Spectropolarimeter (Applied Photophysics). The intensity of scatter light was measured with a fluorescence detector at an

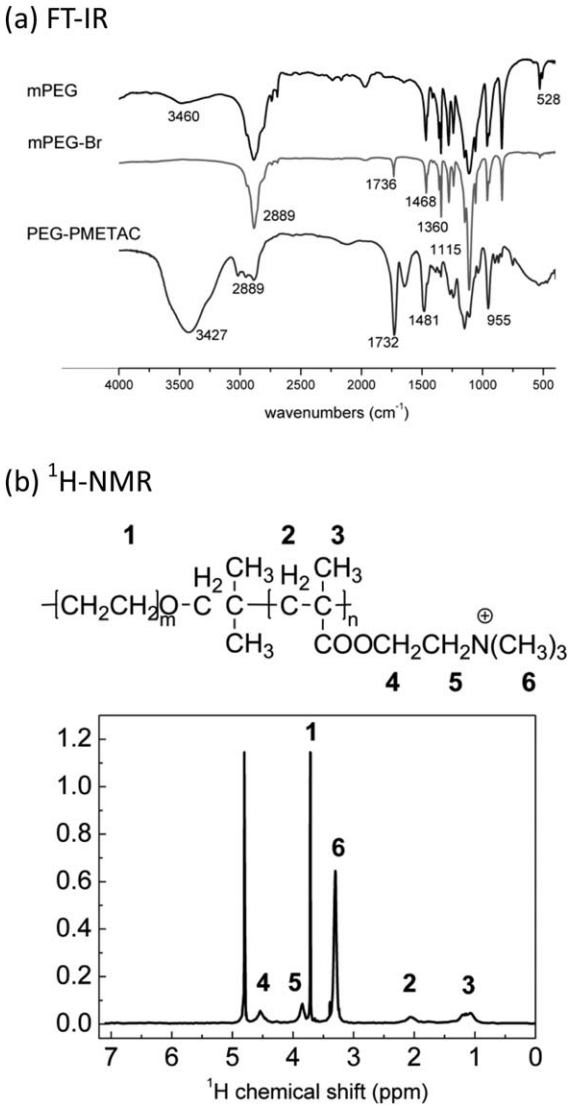

Figure 2. Characterization of mPEG-*b*–PMETAC: (a) FT-IR; (b) 1H-NMR.

excitation wavelength of 577 nm and an excitation voltage of 300 mV.

Fluorescence Spectra of the Mixture Solution. Fluorescence spectra were obtained with an RF-5301 spectrofluorophotometer (SHIMADZU). All measurements were obtained at an excitation wavelength of 280 nm and an emission wavelength range of 280–400 nm at room temperature.

Circular Dichroism Spectra of the Mixture Solution. Circular dichroism (CD) spectra were determined with the Chirascan Spectropolarimeter (Applied Photophysics). All measurements were obtained at a wavelength range of 180–300 nm at room temperature.

RESULTS AND DISCUSSION

Synthesis and Characterization of mPEG-*b*–PMETAC

We chose atom transfer radical polymerization (ATRP) for synthesis of the hydrophilic and positively charged block polymer, mPEG-*b*–PMETAC, due to its strength in the controllable synthesis of polymers with uniform molecular weight and structure.[21] The quaternary ammonium block of this polymer offers electrostatic interaction with the negatively charged protein, and the PEG block offers a hydrophilic and biocompatible microenvironment for the encapsulated protein.

The obtained polymer was subjected to Fourier transform infrared spectroscopy (FT-IR) and ^{1}H nuclear magnetic resonance (^{1}H-NMR). The results of these studies are shown in Figure 2.

Figure 2(a) shows the FT-IR spectrum of mPEG, mPEG-Br, and mPEG-*b*–PMETAC, respectively. Compared to mPEG and mPEG-Br, the peak at 2460 cm^{-1} disappeared and a peak emerged at 1730 cm^{-1}, which indicated the conversion of —OH groups of mPEG to ester groups. The peak at 3427 cm^{-1} indicated hydrogen bonds in residual water. The peak at 2889 cm^{-1} represented methylene or methyl groups. In the mPEG-*b*–PMETAC spectrum, splitting of the peak at 2889 cm^{-1} indicated the existence of both methylene groups in the PEG chains and methyl groups in the PMETAC chains. The peaks between 1461 and 955 cm^{-1} were assigned to the fingerprint region of the PEG chain, and no obvious alterations were detected.

The structure of mPEG-*b*–PMETAC was further confirmed by the ^{1}H-NMR spectrum with D_2O as the solvent, as shown in Figure 2(b). The peak at 4.8 ppm indicated residual water in mPEG-*b*–PMETAC. Peak 1 indicated methylene groups in PEG blocks (*m*, $\delta = 3.72$ ppm, —OCH_2CH_2—); Peak 2 (*s*, $\delta = 2.05$ ppm) and Peak 3 (*m*, $\delta = 1.22$ ppm) represent methylene and methyl groups in the skeleton of the PMETAC block, respectively; Peak 4 (*m*, $\delta = 3.86$ ppm) and Peak 5 (*s*, $\delta = 3.30$ ppm) refer to methyl groups, which were connected to the positively charged nitrogen atom in the quaternary ammonium segments. According to the ratio of the peak area of proton from PEG segments (Peak 1) to that of the quaternary ammonium group (Peak 6) in PMETAC segments, the weight-average molecular weight was calculated and was found to be 11 kDa. GPC analysis of the polymer was unsuccessful as the high surface charge density of the PMETAC block made the polymer extremely hydrophilic and thus insoluble in chloroform or tetrahydrofuran. Aqueous phase GPC was also unsuitable for analysis of polyions such as mPEG-b–PMETAC as the elution may be distorted by the electrostatic interaction, either attractive or repulsive, and thus affects interpretation of the molecular weight of the polyions.[22]

Encapsulation of Insulin with mPEG-*b*–PMETAC Micelles

Encapsulation was conducted by mixing insulin and mPEG-*b*–PMETAC solution at room temperature. During each run, the final concentrations of insulin and mPEG-*b*–PMETAC were 0.034 and 0.34 mM, respectively, i.e., the molar ratio of mPEG-*b*–PMETAC to insulin was 10 : 1.

Determination of the complexation efficiency showed that 96.7% of insulin was encapsulated by mPEG-*b*–PMETAC. Similar studies on insulin complexation with cationic polymers generally obtained a complexation efficiency of 85 to 100%.[14,23,24]

DLS measurements showed that the typical particle size in the mixture solutions varied from 100 to 800 nm under different

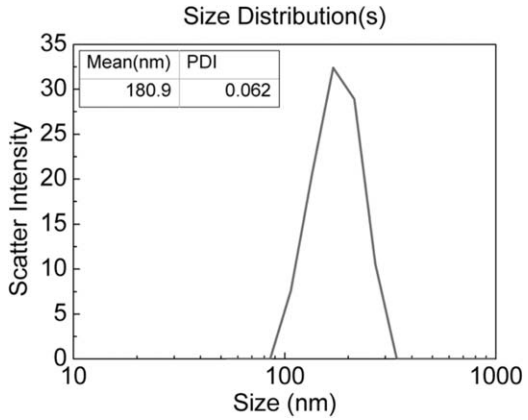

Figure 3. Size distribution of the insulin–mPEG-b–PMETAC assembly.

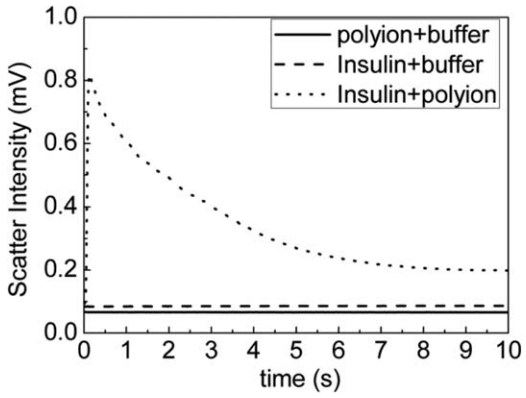

Figure 4. Scatter light intensity of the stop-flow mixture of insulin and mPEG-b–PMETAC.

conditions. The size distribution at pH 7.0 without the addition of NaCl is shown in Figure 3. It was shown that the mixture of insulin and mPEG-*b*–PMETAC formed micelles with a diameter of 180 nm and a narrow distribution, indicating a homogenous structure, which benefitted from the uniform polymer synthesized using ATRP. However, a TEM graph was not obtained because the micelles were only stable in aqueous solution.

The kinetics of the assembly were determined using the stop-flow experiment. Scatter light intensity indicated the number of particles in solution. Figure 4 shows the stop-flow mixture of insulin and mPEG-*b*–PMETAC at pH 7.0.

No significant change in scatter light intensity was observed when insulin or mPEG-*b*–PMETAC was mixed with buffer solution. When insulin was mixed with mPEG-*b*–PMETAC, scatter light intensity rose rapidly within 200 ms, showing that large particles formed in solution due to aggregation of insulin and polyions. The intensity then decreased within 10 s, showing that the initial large particles were unstable and dissociated to form smaller and more stable nanoscale species. The stop-flow experiment conducted under other conditions obtained similar encapsulation kinetics.

Encapsulation of Insulin with mPEG-*b*–PMETAC at Different pH Values

The effect of pH on assembly was investigated. The final concentrations of insulin and mPEG-*b*–PMETAC were 0.034 and 0.34 mM, respectively. During each run, the pH of the final solution was adjusted from 3.0 to 8.0. Table I shows the size of mPEG-*b*–PMETAC, insulin, and the mPEG-*b*–PMETAC/insulin mixture at different pH values, as determined by DLS.

mPEG-*b*–PMETAC is a cationic polyelectrolyte in aqueous solution regardless of pH, while the charge property of insulin molecules is determined by pH. Surface charges of insulin at different pH values, which were calculated using the H++ simulation tool (Supporting Information), are shown in Supporting Information Figure S1 and Table I. The isoelectric point of insulin was around pH 5.5, which is consistent with that obtained in other studies.[25,26]

As shown in Table I, insulin or mPEG-*b*–PMETAC did not produce observable scattering within the detection limits in isolated states. The size of the polymer micelle encapsulating insulin was pH-responsive. When the pH was lower than 5.0, no complex was detected. When the pH was 5.0, loose complexes were formed with a large diameter and a wide distribution, indicating that an incompact structure was formed at the transition state.[27] A higher encapsulation yield and a smaller complex diameter were obtained when the pH of the solution was greater than 5.0. Thus, it was possible to load insulin into the polymer micelles at a neutral or basic pH and discharge insulin at an acidic pH. This was favorable for the stability of encapsulated insulin and prevented cleavage by trypsin or chymotrypsin.

Table I. Hydrodynamic Diameters and Charge Properties of mPEG-*b*–PMETAC/Insulin Complex at Different pHs

pH	Polymer diameter (nm)	Insulin diameter (nm)	Insulin charge[a]	Complex diameter (nm)[b]	Loading efficiency (%)
3.0	ND	ND	3.989	ND	0
4.0	ND	ND	2.283	ND	0
5.0	ND	ND	0.514	314.1 (0.222)	56.3
6.0	ND	ND	−0.757	141.7 (0.084)	95.8
7.0	ND	ND	−2.340	180.9 (0.062)	96.7
8.0	ND	ND	−3.670	175.8 (0.068)	96.3

ND, not detected.
[a] Determined by H++ calculation, details are given in Supporting Information.
[b] The values in brackets indicate the polydispersity index (PDI).

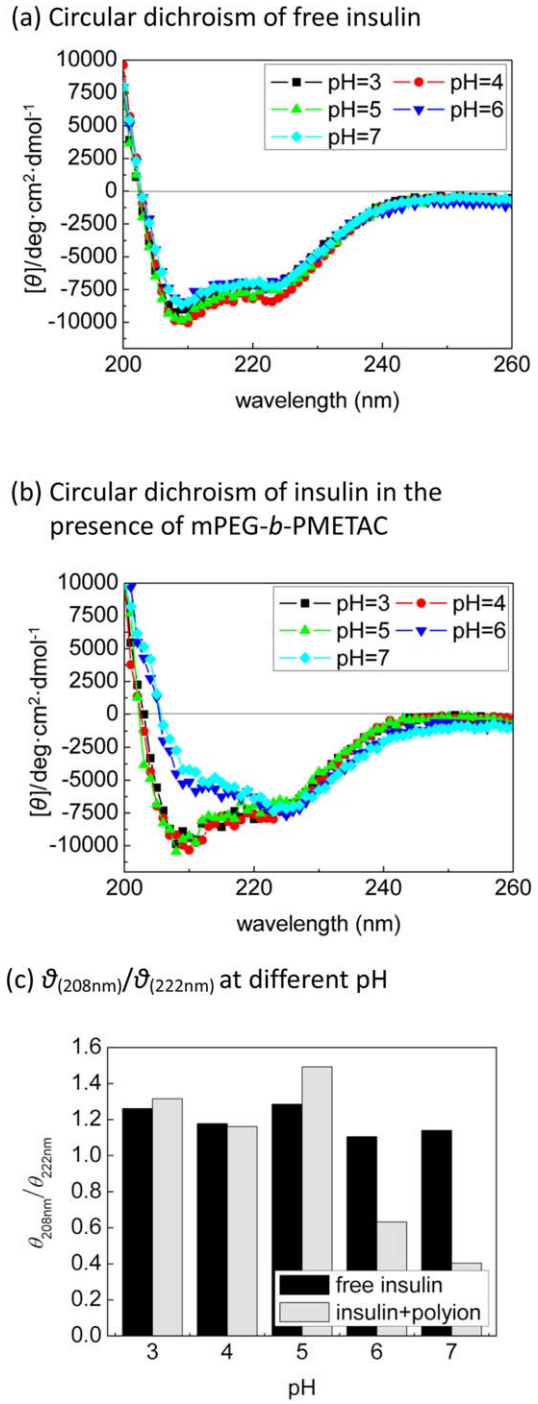

Figure 5. Secondary structure analysis of insulin and its complex at different pH values: (a) circular dichroism of free insulin; (b) circular dichroism of insulin in the presence of mPEG-*b*–PMETAC; (c) θ (208 nm)/θ (222 nm) at different pH values. [Color figure can be viewed in the online issue, which is available at wileyonlinelibrary.com.]

The secondary structures of free insulin and its corresponding complex with mPEG-*b*–PMETAC at different pH values were determined and are shown in Figure 5.

Figure 5(a) shows the circular dichroism (CD) spectra of natural insulin at pH 3.0–7.0. Two natural peaks at 208 and 220 nm

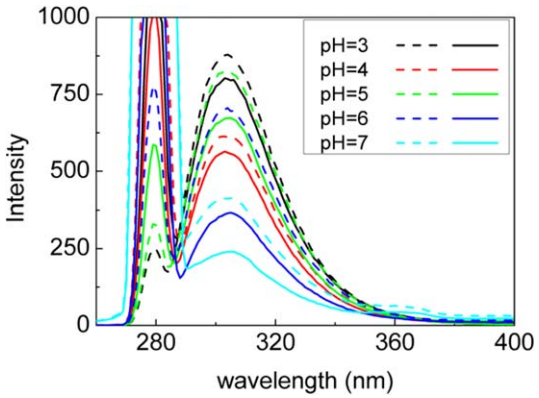

Figure 6. Fluorescence emission spectra of free insulin and its complex at different pH values. **Notes**: Dashed lines show the fluorescence emission spectrum of free insulin; solid lines show the fluorescence emission spectrum of insulin complexed with polyions. [Color figure can be viewed in the online issue, which is available at wileyonlinelibrary.com.]

indicated that the secondary structure of native insulin was composed of three α-helices in chain A and B, and one β-sheet. When molecules aggregate to form dimers or hexamers,[28,29] the residues in the helix of the B chain play important roles.[30] The transition of insulin between monomer and dimers or hexamers is influenced by concentration, pH, and metal ions (Zn^{2+}, etc.). Insulin is prone to aggregate in neutral solution, and forms monomers or dimers at pH 2 or lower, and at pH 9 or higher.[31,32] Therefore, in the pH range of 3.0–7.0, insulin molecules prefer to form hexamers which favor the stability of insulin.

Figure 5(b) shows the CD spectra of insulin in the presence of mPEG-*b*–PMETAC. When the pH was below 6.0, the CD spectra of insulin in the presence of mPEG-*b*–PMETAC was indistinguishable from that of free insulin, indicating that mPEG-*b*–PMETAC had little effect on the secondary structure of insulin at low pH. At pH 6.0 and 7.0, the intensity of the peak at 208 nm, which is the characteristic absorption of the α-helix of insulin, decreased significantly. Considering that the insulin and mPEG-*b*–PMETAC complex was formed at high pH as shown in Table I, this suggests that at pH 6.0 and 7.0, the structural

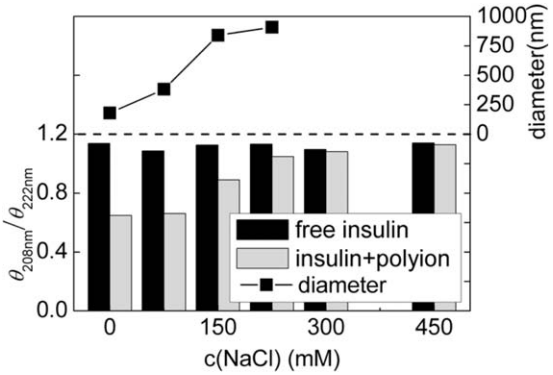

Figure 7. Influence of NaCl concentration on the size* and secondary structure of the insulin–mPEG-*b*–PMETAC complex. **Notes:** No particles were detected when the NaCl concentration was greater than 225 mM.

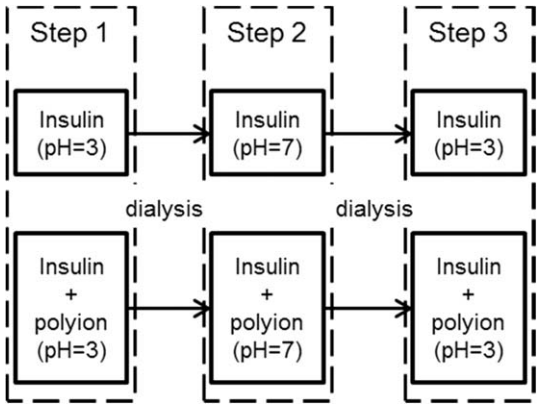

Figure 8. Reversible pH-responsive protocols for the insulin/mPEG-*b*–PMETAC complex.

transition of insulin from α-helix/β-sheet to β-sheet structure occurred during the encapsulation by mPEG-*b*–PMETAC.

In this study, we used $\theta_{(208\ nm)}/\theta_{(222\ nm)}$ to characterize the structure of insulin both in the free and complex state. The influence of pH on the value of $\theta_{(208\ nm)}/\theta_{(222\ nm)}$ is shown in Figure 5(c). When mPEG-*b*–PMETAC was added to insulin solution at pH 3.0–4.0, insulin maintained its natural secondary structure. From the DLS results shown in Table I, no complex was formed under these conditions and the polymer itself had no effect on insulin structure. Although the nanosized complex was detected at pH 5.0 (Table I), insulin in the complex maintained its natural structure. This was due to the loose complex formed between insulin and the polymer with a diameter greater than 300 nm. A further increase in pH value led to a more negative charge on insulin, intensified the electrostatic interaction between insulin and mPEG-*b*–PMETAC, resulted in a more compact complex (Table I) and the structural transition of insulin from α-helix/β-sheet to β-sheet structure.

There are six acidic amino acid residues in an insulin molecule, namely Glu A4, Glu A17, Asn A21, Glu B13, Glu B21, and Thr B30, four of which form parts of the α-helix structure. In solution at high pH, the acidic residues behave as negative charge centers, which can interact with the cationic polymer. Thus, the α-helix structure may be damaged due to the strong interaction between the cationic polymer and insulin, resulting in a significant decrease in the $\theta_{(208\ nm)}/\theta_{(222\ nm)}$ value, as observed.

Figure 6 shows the fluorescence emission spectra of mPEG-*b*–PMETAC/insulin complex and their free counterparts at different pH values.

It can be seen that free insulin exhibited an emission peak at the wavelength of 305 nm when the excitation wavelength was 280 nm, due to lack of tryptophan residues. When encapsulated with mPEG-*b*–PMETAC, this peak intensity at 305 nm significantly decreased. Quenching indicated a strong interaction between insulin and mPEG-*b*–PMETAC, as it is often seen in the electrostatic interaction between proteins and charged polymers.[33] Increased pH led to more fluorescence quenching, indicating the intensity of the interaction between insulin and mPEG-*b*–PMETAC at increased pH. In addition, a red shift in maximum emission wavelength at pH 6.0 and 7.0 was observed, indicating that more hydrophobic groups in insulin were exposed to the aqueous environment caused by extremely hydrophilic mPEG-*b*–PMETAC.[34] In contrast, a red shift was not observed at pH 3.0–5.0.

Encapsulation of Insulin by mPEG-*b*–PMETAC at Different NaCl Concentrations

To examine the effect of ionic strength on the assembly based on electrostatic interaction, the effects of NaCl concentration on the assembly were investigated. The final concentrations of insulin and mPEG-*b*–PMETAC were 0.034 and 0.34 mM, respectively, in each run. The NaCl concentration ranged from 0.0 to 450 mM at pH 8.0.

As shown in Figure 7, the average diameter of the nanoparticles increased from 100 to 900 nm as the NaCl concentration increased from 0 to 225 mM. No nanoparticles were detected when the NaCl concentration was greater than 225 mM. As shown in the circular dichroism spectra, when the salt concentration increased, the value of $\theta_{(208\ nm)}/\theta_{(222\ nm)}$ for the mPEG-*b*–PMETAC/insulin complex increased and approached the

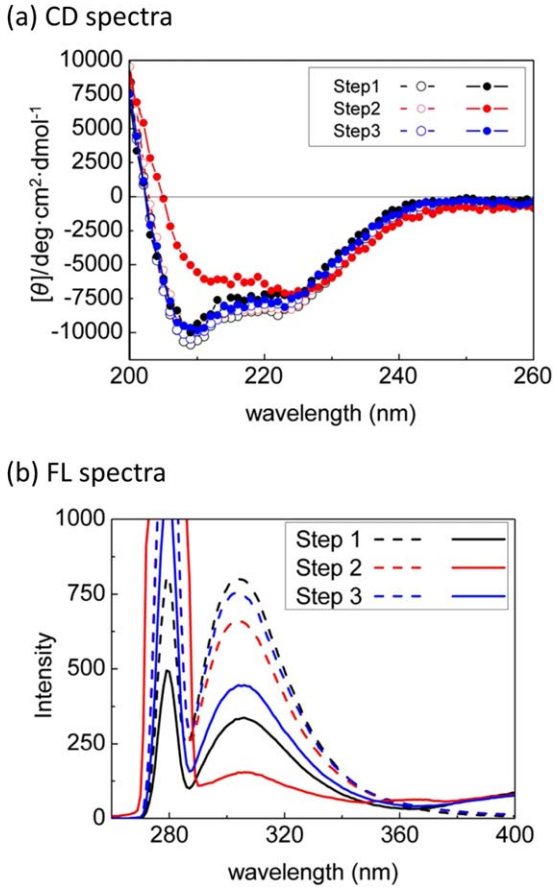

Figure 9. Structural transition of reversible encapsulation under different pH values: (a) CD spectra; (b) FL spectra. **Notes:** Dashed lines show circular dichroism and fluorescence emission spectra of natural insulin; solid lines show spectra of the insulin complex with mPEG-*b*–PMETAC. [Color figure can be viewed in the online issue, which is available at wileyonlinelibrary.com.]

Table II. Reversible Encapsulation of Insulin by mPEG-*b*–PMETAC Triggered by pH Swing

Average particle diameter (nm)			
	Step 1 (pH = 3.0)	Step 2 (pH = 7.0)	Step 3 (pH = 3.0)
Insulin	ND	ND	ND
mPEG-*b*–PMETAC/insulin	ND	175.7 (0.086)[a]	ND
$\theta_{(208\ nm)}/\theta_{(222\ nm)}$			
	Step 1	Step 2	Step 3
Insulin	1.220	1.167	1.279
mPEG-*b*–PMETAC/insulin	1.331	0.656	1.228
Fluorescence ratio of insulin in complex and its free counterpart (F/F_0)			
	Step 1	Step 2	Step 3
F/F_0	0.420	0.231	0.586

ND, not detected.
[a] The values in brackets indicate the polydispersity index (PDI).

value of free insulin at pH 8. When the concentration of NaCl was greater than 225 mM, the $\theta_{(208\ nm)}/\theta_{(222\ nm)}$ for the mPEG-*b*–PMETAC/insulin complex and its free counterpart was not distinguishable. This suggested that an increase in the ionic strength reduced the electrostatic interaction between insulin and mPEG-*b*–PMETAC.

pH-Responsive Assembly of the Insulin–mPEG-*b*–PMETAC

A pH-responsive encapsulation and release of insulin by mPEG-*b*–PMETAC was performed, as shown in Figure 8. Briefly, in step 1, insulin and mPEG-*b*–PMETAC were dissolved in Gly–HCl–NaCl buffer (pH = 3.0, 10 mM) for 12 h. In step 2, this mixture was dialyzed with phosphate buffer (pH = 7.0, 10 mM) for 12 h, and the final pH of the dialyzed solution was tuned to 7.0. In step 3, the obtained solution was dialyzed with Gly–HCl–NaCl buffer (pH 3.0, 10 mM) for 12 h, and the final pH of the dialyzed solution was tuned to 3.0. At each step, samples were collected for CD, FL, and DLS analysis.

The CD spectrum and fluorescence emission spectrum are shown in Figure 9(a and b), respectively. A summary of the results is shown in Table II.

As shown in Table II, no nanoparticles were observed at pH 3.0 both in the free insulin solution and in the insulin/mPEG-*b*–PMETAC solution. When the pH was adjusted to 7.0, nanoparticles composed of insulin and mPEG-*b*–PETAC appeared. In contrast, no such nanoparticles appeared in the free insulin solution. When the pH was tuned to 3.0 again, no nanoparticles of mPEG-*b*–PETAC were detected, indicating dissociation of the insulin–polymer assembly.

The CD spectrum shown in Figure 9(a) and Table II shows that at pH 3.0 (in step 1), the secondary structure of insulin with mPEG-*b*–PMETAC was similar to that of free insulin with the $\theta_{(208\ nm)}/\theta_{(222\ nm)}$ value of 1.22. When the pH of the solution was tuned to 7.0 (in step 2), the formation of the complex driven by electrostatic interaction between negatively charged insulin and positively charged mPEG-*b*–PMETAC occurred, resulting in the structural transition from α-helix/β-sheet ($\theta_{(208\ nm)}/\theta_{(222\ nm)}$ was around 1.22) to β-sheet structure ($\theta_{(208\ nm)}/\theta_{(222\ nm)}$ was around 0.66). When the pH was again tuned to 3.0 (in step 3), the transition from β-sheet structure to α-helix/β-sheet occurred, indicating that this structural transition was reversible. The FL spectrum shown in Figure 9(b) and Table II also demonstrated the reversible tertiary structural transition of insulin on encapsulation and release.

Stability of Encapsulated Insulin Against Enzymatic Degradation

The loss of biological function in protein and peptide drugs *in vivo* is often caused by protease degradation; especially after oral administration where digestive enzymes are encountered.[35] In this study, trypsin and chymotrypsin were used as proteases to degrade the polymer encapsulated insulin, using free insulin as a control. Figure 10 shows the residual intact insulin after enzymatic degradation in the presence and absence of mPEG-*b*–PMETAC at pH 8. Detailed elution curves are shown in Supporting Information (Figure S2).

The content of insulin was calculated from the volume and absorbency of the fraction which appeared at 25 min during elution (Supporting Information Figure S2). As shown in Figure 10, after a 3 h enzymatic degradation period, the contents of residual intact insulin were below 30% in the case of free insulin after both trypsin and chymotrypsin treatment, while those in the case of the insulin/mPEG-*b*–PMETAC complex were

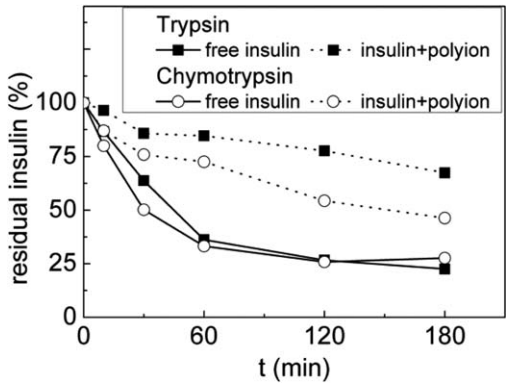

Figure 10. Enzymatic degradation ratio of insulin by trypsin and chymotrypsin.

above 50 and 70%, after chymotrypsin and trypsin treatment, respectively.

Insulin is cleaved by trypsin at B22-B23 and B29-B30 [Supporting Information Figure S3(a)],[20] which are adjacent to the glutamate residue (B21) and the carboxyl at the end position, both of which are negatively charged and thus attract the positively charged blocks of mPEG-*b*–PMETAC chains, and this hindered enzymatic degradation. In addition, the positively charged blocks of mPEG-*b*–PMETAC appear to have an electrostatic repulsive force on the positively charged trypsin molecules (pI = 10.5) at pH = 8. This further inhibited its degradation of insulin. Tsiourvas *et al.* reported that oligolysine or oligoarginine, other types of biocapatible polycations which form complexes with proteins, failed to protect insulin from trypsin degradation.[23]

With regard to chymotrypsin which has 7 cleavage sites on insulin molecules [Supporting Information Figure S3(b)] (5 on the surface and 2 in the hydrophobic core),[20] a more comprehensive inhibition may require a larger mPEG-*b*–PMETAC polymer to shield all cleavage sites. In addition, chymotrypsin with pI of 8.1–8.6 is very weakly charged at pH = 8, thus the electrostatic repulsive force between the polymer and chymotrypsin is much weaker, compared to that between the polymer and trypsin. These factors may account for the reduced degradation by chymotrypsin, as compared to that obtained by trypsin.

CONCLUSIONS

In conclusion, a hydrophilic-cationic diblock copolymer, PEG-*b*–PMETAC, capable of pH-responsive encapsulation of insulin was synthesized. Reversible changes in the secondary and tertiary structure of insulin were observed during the pH-trigged formation and dissociation of the assembly with PEG-b–PMETAC. Significantly enhanced stability against enzymatic degradation by trypsin and chymotrypsin were observed. These findings indicate that this pH-responsive assembly system is promising for the drug delivery of proteins/peptides.

ACKNOWLEDGMENTS

The support from the National Natural Science Foundation of China (No. 21036003 and 21276138) and Tsinghua University Foundation (No. 2013108930) are gratefully acknowledged. Author contributions: Diannan Lu, Zheng Liu, Yifei Zhang, and Zongjun Li conceived and designed the experiments. Zongjun Li and Yifei Zhang performed the experiments. Diannan Lu performed the molecular simulation. All authors discussed the results and co-wrote the manuscript. Disclosure: The author reports no conflicts of interest in this work.

REFERENCES

1. Gillies, E. R.; Frechet, J. M. *J. Pure Appl. Chem.* **2004**, *76*, 1295.
2. Kim, S. K.; Foote, M. B.; Huang, L. *Biomaterials* **2012**, *33*, 3959.
3. Bysell, H.; Mansson, R.; Hansson, P.; Malmsten, M. *Adv. Drug Delivery Rev.* **2011**, *63*, 1172.
4. Kabanov, A. V.; Vinogradov, S. V. *Angew. Chem. Int. Edit.* **2009**, *48*, 5418.
5. Chang, S. F.; Chang, H. Y.; Tong, Y. C.; Chen, S. H.; Hsaio, F. C.; Lu, S. C.; Liaw, J. H. *Hum. Gene Ther.* **2004**, *15*, 481.
6. Ge, J.; Lu, D. N.; Yang, C.; Liu, Z. *Macromol. Rapid Commun.* **2011**, *32*, 546.
7. Bronich, T. K.; Ming, O. Y.; Kabanov, V. A.; Eisenberg, A.; Szoka, F. C.; Kabanov, A. V. *J. Am. Chem. Soc.* **2002**, *124*, 11872.
8. Voets, I. K.; de Keizer, A.; Stuart, M. A. C. *Adv. Colloid Interface* **2009**, *147*, 300.
9. Harada, A.; Kataoka, K. *J. Am. Chem. Soc.* **1999**, *121*, 9241.
10. Van Sluis, R.; Bhujwalla, Z M.; Raghunand, N.; Ballesteros, P.; Alvarez, J.; Cerdán, S.; Galons, J P.; Gillies, R *J. Magn. Reson. Med.* **1999**, *4*, 743.
11. Ghosh, A.; Haverick, M.; Stump, K.; Yang, X. Y.; Tweedle, M. F.; Goldberger, J. E. *J. Am. Chem. Soc.* **2012**, *134*, 3647.
12. Du, C. L.; Deng, D. W.; Shan, L. L.; Wan, S. N.; Cao, J.; Tian, J. M.; Achilefu, S.; Gu, Y. Q. *Biomaterials* **2013**, *34*, 3087.
13. Yudovin-Farber, I.; Yanay, C.; Azzam, T.; Linial, M.; Domb, A. *J. Bioconjugate Chem.* **2005**, *16*, 1196.
14. Thompson, C. J.; Tetley, L.; Uchegbu, I. F.; Cheng, W. P. *Int. J. Pharm.* **2009**, *376*, 46.
15. Lalatsa, A.; Garrett, N. L.; Ferrarelli, T.; Moger, J.; Schatzlein, A. G.; Uchegbu, I. F. *Mol. Pharmaceut.* **2012**, *9*, 1764.
16. Yang, C.; Lu, D. N.; Liu, Z. *Biochemistry-Us* **2011**, *50*, 2585.
17. Wang, Y. H.; Fu, Y. C.; Chiu, H. C.; Wang, C. Z.; Lo, S. P.; Ho, M. L.; Liu, P. L.; Wang, C. K. *J. Nanopart. Res.* **2013**, 15.
18. King, A.; Chakrabarty, S.; Zhang, W.; Zeng, X. M.; Ohman, D. E.; Wood, L. F.; Abraham, S.; Rao, R.; Wynne, K. *J. Biomacromolecules* **2014**, *15*, 456.
19. Schoubben, A.; Blasi, P.; Giovagnoli, S.; Perioli, L.; Rossi, C.; Ricci, M. *Eur. J. Pharma. Sci.* **2009**, *36*, 226.
20. Schilling, R. J.; Mitra, A. K. *Pharma. Res.* **1991**, *8*, 721.
21. Matyjaszewski, K.; Xia, J. H. *Chem. Rev.* **2001**, *101*, 2921.
22. Pfannkoch, E. L. K. C., F. E.; Regnier, H. G.; Barth, H. G. *J. Chromatogr. Sci.* **1980**, *18*, 430.
23. Tsiourvas, D.; Sideratou, Z.; Sterioti, N.; Papadopoulos, A.; Nounesis, G.; Paleos, C. M. *J. Colloid Interface Sci.* **2012**, *384*, 61.
24. Huang, L.; Xin, J. Y.; Guo, Y. C.; Li, J. S. *J. Appl. Polym. Sci.* **2010**, *115*, 1371.
25. Gao, J. M.; Mrksich, M.; Gomez, F. A.; Whitesides, G. M. *Anal. Chem.* **1995**, *67*, 3093.
26. Tanford, C.; Epstein, J. *J. Am. Chem. Soc.* **1954**, *76*, 2163.
27. Voets, I. K.; Fokkink, R.; Hellweg, T.; King, S. M.; de Waard, P.; de Keizer, A.; Stuart, M. A. C. *Soft Matter* **2009**, *5*, 999.

28. Pocker, Y.; Biswas, S. B. *Biochemistry* **1980**, *19*, 5043.
29. Chang, X. Q.; Jorgensen, A. M. M.; Bardrum, P.; Led, J. *J. Biochemistry* **1997**, *36*, 9409.
30. Olsen, H. B.; Ludvigsen, S.; Kaarsholm, N. C. *Biochemistry* **1996**, *35*, 8836.
31. Tokumoto, S.; Higo, N.; Sugibayashi, K. *Int. J. Pharm.* **2006**, *326*, 13.
32. Xu, Y. S.; Yan, Y. F.; Seeman, D.; Sun, L. H.; Dubin, P. L. *Langmuir* **2012**, *28*, 579.
33. Cooper, C. L.; Dubin, P. L.; Kayitmazer, A. B.; Turksen, S. *Curr. Opin. Colloid Int.* **2005**, *10*, 52.
34. DeLaLuz, P. J.; Ackley, B. L. *FASEB J.* **2009**, 23.
35. Yun, Y.; Cho, Y. W.; Park, K. *Adv. Drug Delivery Rev.* **2013**, *65*, 822.